KSTLE International Journal, Vol. 8, No. 1, June 2007, pp. 16-20

A Novel Viscosity Measurement Technique Using a Falling Ball Viscometer with a High-speed Camera

Won Jin Jo*, Bock Choon Pak,† and Dong Hwan Lee****

*Graduate student, Department of Mechanical Design, Chonbuk National University, Jeonju, Korea
**Division of Mechanical and Aerospace System Engineering, Chonbuk National University, Jeonju, Korea

Abstract: This study introduces a new approach to a falling ball viscometer by using a high speed motion camera to measure the viscosity of both Newtonian and non-Newtonian fluids from the velocity-time data. This method involves capturing continuous photographs of the entire falling motion of the ball as the ball accelerates from the rest to the terminal velocity state. The velocity of a falling ball was determined from the distance traversed by the ball by examining video tape frame by frame using the marked graduations on the surface of the cylinder. Each frame was pre-set at 0.01. Glycerin 74% was used for Newtonian solution, while aqueous solutions of Polyacrylamide and Carboxymethyl Cellulose were for non-Newtonian solutions. The experimental viscosity data were in good agreements with the results obtained from a rotating Brookfield viscometer.

Keywords: Falling ball viscometer, high speed motion camera, newtonian fluid, non-newtonian fluid, terminal velocity, viscosity

1. Introduction

Falling ball viscometer has been used to measure the viscosity of highly viscous fluids by measuring the terminal velocity [1]. Terminal velocity measurement in a low viscous fluid with the falling ball viscometer is a difficult task if one uses a manual method with a stopwatch because the time lapse for the ball to pass through a given interval in the cylinder is too short to measure accurately [2]. Although the falling ball viscometer has been widely utilized to determine the viscosity of Newtonian fluids because of its simple theory and low fabrication cost, other difficulties still arise [2,3]. One of the drawbacks of using a conventional falling ball viscometer is that one needs to change the density of the ball or the ball size in order to measure the viscosity at different shear rates. Thus, the viscosity can only be measured at a single shear rate at a time. In addition, when the ball falls through the fluid it disturbs the initial stress-free condition of the fluid. This implies a large lag time needed for the fluid to return to its initial stress-free condition before another test can be made. Hence, this conventional method is time consuming and not suitable for practical viscosity measurements.

The objective of the present study is to develop a new viscosity measuring technique using a falling ball viscometer with a high-speed camera. This innovative technique determines viscosity from the distance-time flow curve generated by the falling ball. Thus, unlike the conventional falling ball method, the fluid viscosity can be determined continuously over a range of shear rate at once without having to vary the density and size of a ball.

†Corresponding author; bcpak@chonbuk.ac.kr
Tel: +82-63-270-2454; Fax: +82-63-270-2460

2. Materials and Method

2.1. Description of falling ball viscometer

Figure 1 shows a schematic diagram of the falling ball viscometer, which consists of two concentric plexiglass cylinders, a constant temperature water bath and circulator, a drainage valve, a high speed camera, and a personal computer with frame analysis program (X-Vision, DANTEC DYNAMICS). The inside diameter and height of the cylinder were 10 cm and 64 cm, respectively. The inner cylinder was of a sufficient size so that wall effects could be neglected. The size of the cylinder walls affect the velocity at which the sphere falls. However, previous studies found out that this wall effect is independent of the absolute radius of the ball and cylinder when the ratio of the sphere radius to cylinder radius is considerably less than a certain empirical value. Cho [2] reported that velocity formula might be applicable to all Newtonian, purely viscous, weakly viscoelastic and highly viscoelastic fluids in the range of

$$\frac{R}{R_c} \leq 0.08 \tag{1}$$

If Eq. (1) will be satisfied, wall effects can be neglected. Therefore, in this study, the cylinder radius was determined in range.

Two outside surface of the cylinder was marked with graduations in a millimeter scale. At the base of the cylinder, a balls retrieval section was installed for easy recovery of balls. Since the viscosity measurement from the falling ball viscometer is very sensitive to the temperature changes in the flow field inside the test cylinder, a thermal plexiglass jacket surrounded the test cylinder. The temperature controlled water coming from the constant temperature bath and circulator was supplied to the jacket to ensure that the temperature in the flow field

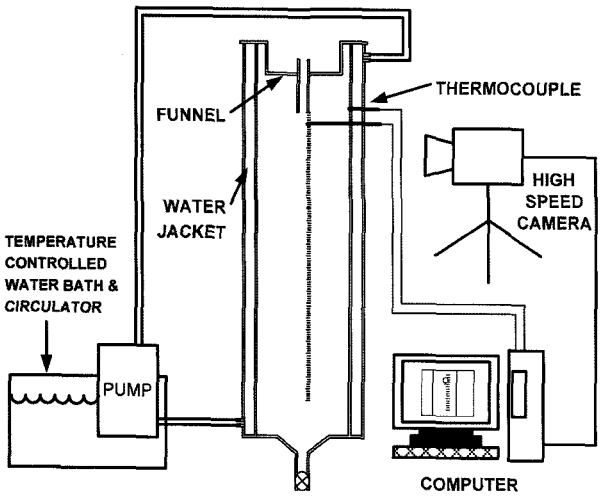

Fig. 1. Schematic diagram of the present falling ball viscometer system.

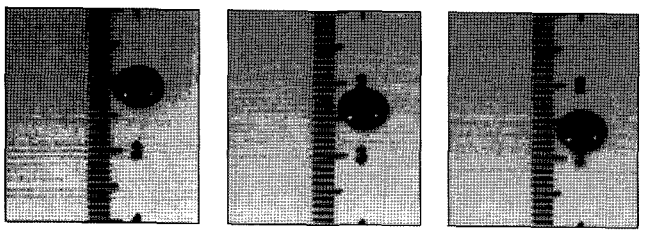

t=0.22s t=0.23s t=0.24s

Fig. 2. A sequence of continuous images of a falling ball captured with a high-speed camera.

stays at a prescribed temperature during the whole experiment. This temperature was monitored by two thermocouples connected to the center and wall of the inner cylinder. The two connections were aimed to keep tract of the possible temperature difference between the fluids near the wall and center of the cylinder as a consequence of considerable cylinder size. Tests were performed when the recorded temperatures from the two probes were accorded 25°C.

A submerged concentric funnel was used at the top of the test cylinder to guide the balls to fall along the center of the cylinder. It also prevented the attachment of air bubbles on the surface of the ball, a condition that would have given erroneous values in the terminal velocity measurement. A high speed camera (X-Stream XS-4, DANTEC DYNAMICS) was used, which was capable of capturing up to 4,000 frames and digitally storing the captured images for convenient playback and further analyses. Figure 2 shows captured images of a falling ball as an example.

2.2. Experimental procedure

Prior to actual tests, the present system was allowed to reach 25°C using a constant temperature bath and circulator. Balls were put in a submerged funnel at the top of the cylinder at a considerable time before tests to eliminate any air bubbles attached on the surface of the balls and to obtain the same temperature as the test liquid. Silundum (SiC) balls were used with a diameter of 0.57 cm and a density of 3.2 g/cm^3. The liquids used were: glycerin (74%, J.T. Baker Co.) for Newtonian fluid, and aqueous solutions of Carboxymethyl Cellulose (CMC 0.5% and 0.7%, Acros Co.) for purely-viscous non-Newtonian fluids, and Polycarylamide (PAM 1%, 2%, Acros Co) for viscoelastic non-Newtonian fluids. During the experiment, the transient displacement was determined from capturing images of its instantaneous position from the initial state to the terminal state and tracking the distance traversed by it using video movie frames along with marked graduations on the falling ball cylinder. The transient velocity was calculated from the derivative of the transient displacement data, from which the terminal velocity was determined. Each frame was pre-set at 0.01 seconds.

Viscosity of each test fluid was also measured using a rotating viscometer (Brookfield Co. DV-III Rheometer) for the comparison of the present experimental data.

2.3. Data reduction

When the ball is dropped from its initial resting state it starts to accelerate due to the force unbalance between the drag force, the buoyant force, and the weight of the falling body. This effect, however, vanishes as the body approaches the terminal velocity in which the falling body attains a constant velocity. The force balance on the sphere at terminal state can be described as follows:

Terminal state:

$$\Sigma F = Weight - F_D - F_B = 0 \tag{2}$$

$$\Sigma F = \rho_b g\left(\frac{\pi}{6}D^3\right) - \frac{C_D V_\infty^2 \rho A}{2} - \rho_f g\left(\frac{\pi}{6}D^3\right) = 0 \tag{3}$$

where F_D and F_B are the drag and buoyancy forces, respectively. When utilizing Stokes' law, F_D can be expressed as $6\pi\mu R V_\infty$. Stokes' law is valid when the Reynolds Number is less than 1.0.

From the force balance equation at the terminal state as shown in Eq. (3), values of the drag force, C_D, are determined from the measured terminal velocity given by,

$$C_D = \frac{4gD(\rho_s - \rho)}{3\rho V_\infty^2} \tag{4}$$

Numerous attempts have been made to establish theoretical relationships of the terminal falling velocity of solid spheres but the theoretical and semi-theoretical expressions are normally only valid for Re <1. For higher Re, resorts are directed toward experimental and empirical relationships. The standard approach is through an empirical expression relating the drag coefficient C_D to the particle Reynolds number Re. Several of these correlations are given below:

In order to determine the correlations covering the entire Re range, a simpler correlation has been proposed by Heider and Levenspiel [4] that was derived from non linear regression using 408 available experimental data points. The final form of the equation was,

$$C_D = \frac{24}{\mathrm{Re}}[1 + 0.186\mathrm{Re}^{0.6459}] + \frac{0.4251}{1 + 6880.95/\mathrm{Re}} \quad (5)$$

$\mathrm{Re} < 2.6 \times 10^5$

Data of Lali *et al.* [5] correlated very well with the Newtonian and non-Newtonian curve defined by,

$$C_D = \frac{24}{\mathrm{Re}}[1 + 0.15\mathrm{Re}^{0.687}] \quad (6)$$

$0.1 < \mathrm{Re} < 10^3$

Mpandelis *et al.* [6] attempted a derivation of an equation similar to Eq. (5) using non linear regression and derived the following equation for the total of 80 points,

$$C_D = \frac{24}{\mathrm{Re}}[1 + 0.1466\mathrm{Re}^{0.378}] + \frac{0.44}{1 + 0.2635/\mathrm{Re}} \quad (7)$$

$0.1 < \mathrm{Re} < 10^3$

Fitting all the available Newtonian and non-Newtonian data, a total of 1148 pairs, in the form of Eq. (5) Mpandelis *et al.* [6] also derived,

$$C_D = \frac{24}{\mathrm{Re}}[1 + 0.1407\mathrm{Re}^{0.0618}] + \frac{0.2118}{1 + 0.4215/\mathrm{Re}} \quad (8)$$

$0.1 < \mathrm{Re} < 10^3$

The most common approach taken by previous investigators for predicting the terminal velocity is through the use of 'standard' Newtonian relationships (C_D –Re) but using modified (non-Newtonian or generalized) Reynolds number.

For power law fluids, the generalized Reynolds number is defined as

$$\mathrm{Re}_{gen} = \frac{\rho V^{2-n} D^n}{m} \quad (9)$$

This definition stems from the standard definition of the Reynolds number given by

$$\mathrm{Re} = \frac{\rho V D}{\mu} \quad (10)$$

For non-Newtonian fluids, instead of using the Newtonian viscosity (μ), apparent viscosity (η) is used. For the power-law fluid, the apparent viscosity is defined as:

$$\eta = \frac{\tau}{\dot{\gamma}} = \frac{m\dot{\gamma}}{\dot{\gamma}} = m\dot{\gamma}^{n-1} \quad (11)$$

The appropriate average shear rate for the case of falling solid spheres in liquids over the entire particle surface is assumed as

$$\dot{\gamma} = \frac{V}{D} \quad (12)$$

Combination of Eq. (11) and Eq. (12) gives

$$\eta = m\left(\frac{V}{D}\right)^{n-1} \quad (13)$$

Finally, substitution of Eq. (13) in Eq. (10) gives Eq. (9) for the generalized Reynolds number.

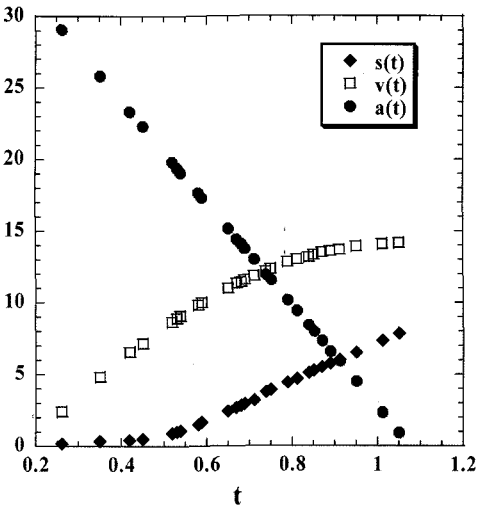

Fig. 3. Distance, Velocity and Acceleration during accelerate state.

3. Results and Discussion

The present falling ball viscometer was based on the determination of the terminal velocity, the power-law index n, and the flow consistency index m from the generated flow curve (distance vs. time) taken from the captured images of the falling ball. From this curve, both velocity and acceleration were obtained by simple differentiation of the gathered data.

Figure 3 shows typical examples of the distance, velocity, and acceleration curves with respect to traverse time from the resting position in case of using CMC as the test fluid. Terminal velocity was the point when the velocity reached the maximum value and remained constant, which corresponds to zero acceleration.

With known terminal velocity, V_∞, and physical properties of both the liquid and the solid sphere, C_D was calculated using Eq. (4). Re was deduced from C_D – Re correlations given by Eqs. (5)~(8). The obtained Re was then used in Eq. (9) to extract the constants m and n. This was done from the curve fitting using a non-linear least square technique. From the power-law model constants m and n, Eq. (13) finally gave the viscosity of the fluid.

Figure 4 shows viscosity results for Glycerin 74% at 25°C obtained with the present falling ball viscometer. The power-law index of the Glycerin 74% was determined to be 1.0 by a computer program (Excel-solver) using Eq. (5), confirming that it was a Newtonian fluid. Based on the present viscosity measurement method, the viscosity of the Glycerin 74% was found to be about 31cP at 25°C. It was evident that the experimental data for Glycerin 74% using the present falling ball viscometer agreed well with the rotating viscometer method. The percentage difference for Glycerin was 0.48%.

Figure 5 illustrate the apparent viscosity of CMC at 25°C, which was measured with both the present viscometer and the cone-and plate rotating viscometer (DV-III) using the above mentioned method. The C_D – Re correlation that yielded the least percentage difference was chosen to represent the falling

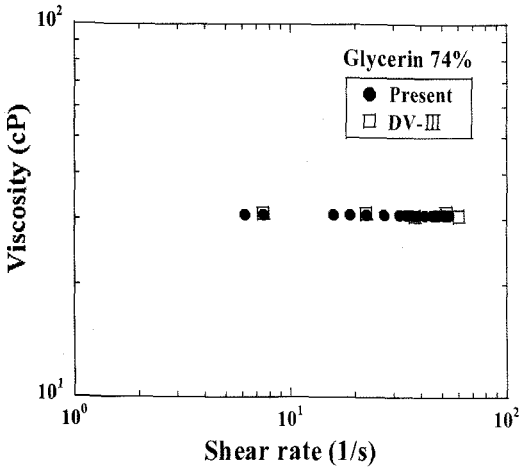

Fig. 4. Viscosity vs. shear rate for Glycerin 74% at 25°C.

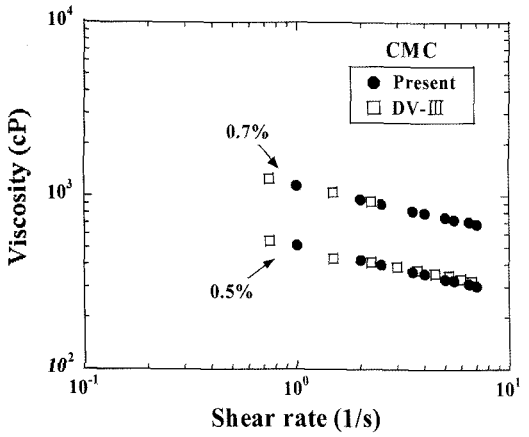

Fig. 5. Apparent viscosity vs. shear rate for aqueous solutions of carboxymethyl cellulose at 25°C.

ball viscometer data. Equation (7) was used for CMC. The viscosity of the CMC measured with the present viscometer was based on a calculation method that determined the power-law index, n, and consistency index, m. The values of n and m were 0.723 and 5.198 for CMC 0.5% whereas n and m for CMC 0.7% were 0.738 and 11.499, respectively.

Moreover, the results showed good shear-thinning behavior. The apparent viscosity decreased with the increase in shear rate. In addition, the viscosities ranged from 300 to 520cP for CMC 0.5% and from 710 to 1150cP for CMC 0.7%, respectively. Therefore it could be confirmed that the change of viscosity depends on the concentration of the fluid. Compared with the measured data using the DV-III, the present test results gave excellent agreement with those measured by the DV-III. The corresponding percentage differences for 0.5% and 0.7% CMC were 3% and 0.6%, respectively.

Figure 6 shows the apparent viscosity of the PAM at 25°C. Compared with the measured data using the DV-III, the test results obtained with the present viscometer gave less than 3% and 1.8% error in the experimental range of shear rate, validating the test methods and data reduction procedure. Based on Eq. (6), the PAM viscosity was estimated to be 21-

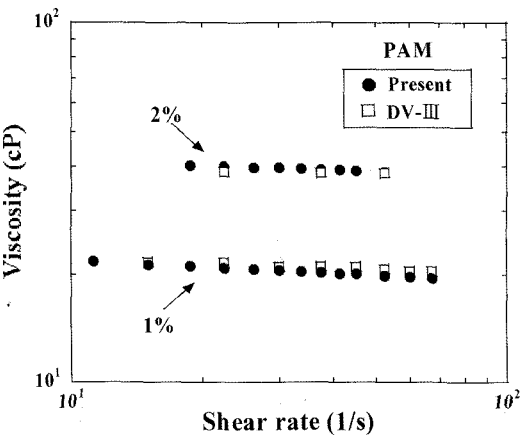

Fig. 6. Apparent viscosity vs. shear rate for aqueous solutions of Polyacrylamide at 25°C.

19cP and 40-39cP for PAM 1% and 2% at 25, respectively. Viscosity data tend to approach a constant value as shear rate decreases. The values of power law index, n were 0.943 and 0.959 for PAM 1% and 2%, respectively. These values were almost equal to 1.0, a parameter applicable for Newtonian fluid. These results might be due to the used of small molecular weight of the PAM powder. Shear thinning behavior can be clearly attained through use of higher molecular weight of PAM powder.

4. Conclusion

The present study introduced a new method of measuring both Newtonian and non-Newtonian fluid viscosities over a range of shear rates. A high speed camera and video imaging method was used to measure the terminal velocity which was too large to measure with a stopwatch technique. Power-law model constants were determined from the drag coefficient for intermediate Re cases. The feasibility and accuracy of the viscosity measurement technique have been demonstrated for 74% glycerin, CMC, and Polyacrylamide by comparing the present results against a rotating viscometer.

Nomenclature

A	The ball frontal area
C_D	Drag coefficient, eq. (4)
D	Diameter of sphere
D_c	Diameter of cylinder
F	Net force on the ball
g	Gravitational constant
m, n	Power-law model constants
R	Radius of sphere
R_c	Radius of cylinder
Re	Reynolds number with constant viscosity, eq. (10)
Re_{gen}	Generalized Reynolds number, eq. (9)
V_∞	Terminal velocity

Greek letters

$\dot{\gamma}$	Shear rate

η Apparent viscosity, eq. (11)
μ Newtonian viscosity
ρ Density of fluid
ρ_s Density of sphere

References

1. Cho, Y. I., Hartnett, J. P., and Lee, W. Y., "Non-Newtonian viscosity measurements in the intermediate shear rate range with the falling ball viscometer," Journal of Non-Newtonian Fluid, Vol. 15, pp. 61-74, 1984.
2. Cho, Y. I., "The Study of Non-Newtonian Flows in the Falling Ball Viscometer," Ph.D. Thesis, University of Illinois, Chicago Circle, 1979.
3. Jeon, C. Y., Hwang, T. S., and Yoo, S. S., "Measurements of viscosity and characteristic times of viscoelastic fluids with the falling ball viscometer and capillary tube viscometer," The Korean Journal of Rheology, Vol. 2, No. 2, pp. 19-27, 1990.
4. Heider, A. and Levespiel, O., "Drag Coefficient and Terminal Velocity of Spherical and Nonspherical Particles," powder Techn, Vol. 58, pp. 63-70, 1989.
5. Lali, A. M., Khare, A. S., Joshi, J. B., and Migam, K. D. P., "Behavior of Solid Particles in Viscous non-Newtonian Solutions: Falling Velocity, Wall Effects and Bed Expansion in Solid-Liquid Fluidized Beds," powder Techn, Vol. 57, pp. 47-77, 1989.
6. Mpandelis, G. E. and Kelessidis, V. C., "New approaches for estimation of terminal settling velocity of solid spheres falling in Newtonian and non-Newtonian fluids," paper presented at the 7th National Congress on Mechanics, 2004.